XANES spectroscopy using high-resolution resonant Raman scattering: application to holmium

1992 J. Phys.: Condens. Matter 4 879

(http://iopscience.iop.org/0953-8984/4/3/027)

J. Phys.: Condens. Matter 4 (1992) 879–886. Printed in the UK

XANES spectroscopy using high-resolution resonant Raman scattering: application to holmium

V Eteläniemi†, K Hämäläinen‡, S Manninen† and P Suortti§

† University of Helsinki, Department of Physics, Helsinki, Finland
‡ NSLS, Brookhaven National Laboratory, Upton, NY 11973, USA
§ ESRF, BP 220, F-38043 Grenoble, France

Received 8 May 1991, in final form 25 September 1991

Abstract. The use of resonant Raman scattering at x-ray energies for studies of the near-edge structure of the absorption edge is presented. The potential of the method is shown in the case of the Ho L_{III}-edge, which is measured using Cu Kα1 radiation and a focusing crystal spectrometer. The results are interpreted within a model where the density of final electron states is constant plus a narrow band where the density is high (white line). A comparison with the other methods used in x-ray absorption near-edge structure spectroscopy is also given.

1. Introduction

The fine structure in the x-ray absorption edge yields information about the density of the unoccupied electron states (x-ray absorption near edge structure XANES) and the coordination of a particular atom (extended x-ray fine structure EXAFS). Originally EXAFSs were measured by scanning the incident photon energy across the absorption edge and measuring the absorption of x-rays when they penetrate through the sample. Later an energy dispersive technique, in which the absorption of the desired energy band is recorded simultaneously, was also used. The alternative way, often used when homogeneous samples are difficult to prepare, is to detect the fluorescence EXAFS or XANES which follows photoelectric absorption. Choosing the best method depends on the sample properties; one should notice, however, that the energy dispersive technique cannot be used in fluorescence EXAFS. These and other EXAFS methods have been reviewed by Stern (1986).

In the case of light elements the use of the conventional EXAFS technique is difficult. The absorption edge energies are then so small that both the absorption method, which requires ultrathin samples, and the fluorescence method, which involves detection of very low x-ray energies, face severe practical problems. One way to avoid this is to measure the differential cross section of inelastic scattering, related to the non-resonant A^2 term in the interaction Hamiltonian, not to the resonant $p \cdot A$ as in EXAFS or fluorescence EXAFS. The absorption edge occurs at the energy $\hbar\omega_1 - E_{\text{bind}}$, where $\hbar\omega_1$ is the energy of the incident photon and E_{bind} the relevant absorption edge energy. In the experiment the primary photon energy does not change, but the energy spectrum of the scattered photons is measured using a high-resolution spectrometer. This makes it possible to work at optimized x-ray energies without

0953-8984/92/030879+08$03.50

the limitations involved in conventional EXAFS. The potential of this technique has recently been demonstrated for diamond and graphite by Tohji and Udagawa (1989) and for Li, Be and graphite by Nagasawa *et al* (1989).

In this work we present another alternative to studying the XANES structure. Below the relevant absorption edge there is a possibility of electron excitation although the energy of the x-ray photon is less than the electron binding energy. This so-called resonant Raman scattering (RRS) is a second-order process involving a virtual intermediate state with a hole in an inner shell. This hole is filled with an electron from an outer shell and the excess energy in this two-step process is shared with the outgoing photon and the excited electron (Sparks 1974, Manninen *et al* 1986, Hämäläinen *et al* 1989). By measuring the resulting energy spectrum using incident photon energies close but below the absorption edge the final electron state densities can be probed. In this case the binding energy of the outer shell electron ($E_{b,2}$) defines the position of the edge of the RRS spectrum relative to the incident energy, $\hbar\omega_2 \leqslant \hbar\omega_1 - E_{b,2}$.

An ideal x-ray source in RRS measurements is the synchrotron, because the energy of the incident beam can be optimized in an XANES type of experiment. There are, however, cases where the energy of the absorption edge is close enough to some particular characteristic x-ray energy. In this work we have studied the L_{III}-edge of holmium using Cu Kα1 radiation, the edge is 23 eV above the incident photon energy. The RRS spectrum is measured using a focusing crystal spectrometer, with an energy resolution of about 10 eV. The observed XANES structure which is almost completely dominated by the white line is compared with a recent fluorescence XANES experiment (Hämäläinen *et al* 1989), made using synchrotron radiation. The differences are interpreted in terms of the corresponding cross sections and also using model calculations with a proposed density of final states.

2. Theory

The theory of RRS has been reviewed recently by Åberg and Tulkki (1985) and several expressions directly applicable to cross-section measurements have been given by Hämäläinen (1990). An illustrative semiclassical presentation of RRS has been put forward by Hämäläinen *et al* (1989). Basically, the RRS is given by the $p \cdot A$ term of the interaction Hamiltonian of an electron and radiation field. One of the terms in the second-order perturbation expansion of the scattering cross section becomes resonant when the energy of the incident photon approaches the binding energy of a core electron. In the case of the KL resonance this term in the dipole approximation is

$$\frac{d\sigma}{d\omega_2} = \frac{r_0^2}{4}\frac{\omega_2}{\omega_1}\frac{\Omega_{KL}(\Omega_{KL}+\omega)g_{KL}}{\hbar(\Omega_{KL}-\omega_2)^2+\Gamma_K^2/4\hbar^2}\left(\frac{dg_K}{d\epsilon}\right)_\epsilon \tag{1}$$

where $r_0 = e^2/mc^2 = 2.818 \times 10^{-5}$ Å is the classical radius of electron, ω_1 the angular frequency of the incident photon and ω_2 that of the scattered photon, $\hbar\Omega_{K,L} = E_L - E_K$ the KL-fluorescence energy, $\epsilon = \hbar\omega = \hbar\omega_1 - \hbar\omega_2 + E_L$ the energy of the ejected electron and Γ_K the lifetime width of the K-shell energy. The oscillator strength of the KL transition is given by g_{KL}, and $(dg_K/d\epsilon)$ is the oscillator density for the transition to the final electron states. The oscillator density is proportional

to the density of electron final states, $dN/d\epsilon$, and the matrix element between the initial and final states $|a\rangle$ and $|b\rangle$,

$$\left(\frac{dg}{d\epsilon}\right)_\epsilon = \frac{2}{m\omega_1}\left(\frac{dN}{d\epsilon}\right)_\epsilon \int d\Omega\, |\langle b|\hat{e}_k \cdot p|a\rangle|^2 \tag{2}$$

Here m is the electron mass, $\hat{e}_k$ the polarization unit vector of the photon with the wavevector k and p the electron momentum. The oscillator density is related to the total absorption cross section $\sigma(\omega_1)$ by

$$\sigma(\omega_1) = 2\pi r_0^2 c \left(\frac{dg}{d\epsilon}\right)_{E_K+\hbar\omega_1} \tag{3}$$

The total cross section of the RRS is found by an integration over transitions to the states with $\epsilon > 0$,

$$\sigma(\omega_1) = \frac{\Gamma_K}{2\pi\hbar\omega_1\Omega_{KL}} \int_0^{\omega_1+E_L/\hbar} d\omega_2\, \frac{\omega_2(\Omega_{KL}+\omega_1-\omega_2)\sigma(-E_K+\epsilon)}{(\Omega_{KL}-\omega_2)^2+\Gamma_K^2/4\hbar^2}. \tag{4}$$

The differential cross section (1) is essentially a Lorentzian with a FWHM of $\Gamma_K/\hbar$, centred at Ω_{KL} and modulated by $(dg_K/d\epsilon)$. Because of the limitation $\epsilon \geqslant 0$, only the part $\omega_2 \leqslant \omega_1 + E_L/\hbar$ is excited. When $\omega_1 + E_K/\hbar \geqslant \Gamma_K/\hbar$, full fluorescence results. The Lorentzian of (1) is convoluted by the Lorentzian of an L-shell level, so that the width of the fluorescence line is $\Gamma_K + \Gamma_L$. When ω_1 is scanned the modulations of $(dg_K/d\epsilon)$ move through the centre of the fluorescence line ($\omega_2 = \Omega_{KL}$) and even $\sigma(\omega_1)$ is substantially affected. Accordingly, the oscillator density, convoluted with the Lorentzian of the K-shell hole, is obtained from the absorption coefficient or the intensity of fluorescence. The structures seen in either one are called XANES or EXAFS.

When $\omega_1 - E_K/\hbar \leqslant -\Gamma_K/\hbar$ only the upper tail of the Lorentzian distribution of the K-shell contributes. The spectrum of the scattered radiation has the shape of this tail, modulated by $(dg_K/d\epsilon)$ and convoluted by the L distributions. This convolution makes the RRS spectrum a superposition of the components corresponding to the transitions from L_{II} and L_{III}. The modulations due to $(dg_K/d\epsilon)$ have been observed in the RRS of Cu Kα1 radiation from Ni, although much of the modulations are damped by the superposition of the K L_{II} and K L_{III} spectra (Suortti *et al* 1987). Provided that the spectrum can be decomposed the features of $(dg_K/d\epsilon)$ are resolved better than in XANES or EXAFS, because the RRS spectrum is convoluted by the higher-shell distribution only and not by the broader Lorentzian of the K shell. Fine details of the density of states and local environments of the resonant atom can be probed, which is particularly important in studies of magnetic contributions to resonant scattering.

3. Experiment

The measurements were made on a Ho foil supplied by Goodfellow Ltd, UK. A conventional fine focus x-ray tube running at 40 kV and 30 mA was used and the Johansson type quartz (10 · 1) monochromator focused the Cu Kα1 component to

a narrow line on the sample. The scattered radiation was analysed by a Johann type spherically bent Si(220) crystal (bending radius 0.8 m) moving the analyser and the detector (NaI scintillation counter) simultaneously while keeping the scattering angle constant. The sample, the analysing crystal and the detector were all on the Rowland circle and the symmetrical reflection geometry was maintained by coupling them to the centre of that circle. The energy scale was based on the positions of the Ho L_{III}-fluorescence lines, excited by harmonic energies and K-fluorescence lines of Co, measured separately. The details of this type of spectrometer have been given previously (Pattison *et al* 1986, Suortti *et al* 1986, 1987).

The RRS scattering cross section depends on the energy of the incident radiation relative to the binding energy of the desired inner shell. Far from the edge the cross section is too small, and close to the edge the line shape is too sharp (it approaches the fluorescence line shape) making the separation of the fine structure difficult. Based on our earlier experience, the energy difference 23 eV between the Ho L_{III} edge (8.071 keV, Bearden and Burr 1967) and Cu Kα1 radiation is close to the optimum for RRS fine structure studies. According to the dipole selection rules the possible transitions from the M shell to the L_{III}-subshell include either 3s or 3d electrons. Because of the larger number of the 3d electrons (and therefore larger cross section) $M_{IV,V}$–L_{III} transition was selected. The edge positions are therefore at $\hbar\omega_1 - E_{bind}(M_{IV,V})$, i.e. about 1400 eV below the incident energy. One should note that there are two edges, at 6.656 and 6.697 keV, related to M_{IV} and M_V, respectively. The separation of these overlapping contributions is, however, straightforward because the energy separation (41 eV) and the intensity ratio (100:11.1) are known. The resolution of the spectrometer at the energy range of interest was determined using Co Kα-fluorescence, Kα1 = 6.930 keV (Bearden 1967), and it turned out to be about 10 eV. It should be noted that the resolution in this type of spectrometer depends on the beam size at the sample, seen by the analysing crystal, and it therefore depends on the sample thickness and absorption.

Because the white line is the dominant feature in the XANES spectrum of Ho, finer steps (2 eV) were used close to the white line and the other parts of the scattered RRS spectrum were measured using 5 eV steps. The energy range used in the experiment was 210 eV and the total measuring time for each point was 3500 s. Also the whole energy range from Cu Kα1 to the desired RRS spectrum was measured using 5 eV steps to estimate the background level and to calibrate the energy scale. The experimental data including both L_{III} M_{IV} and L_{III} M_V components is shown in figure 1.

The data were corrected for the background absorption in the sample and in the air and for the change of the solid angle seen by the detector due to the moving receiving slit. The change in the analyser crystal efficiency within the small energy range used in the analysis and the absorption in the detector window were not taken into account. After these corrections the contribution of the overlapping L_{III} M_V component was removed using the known intensity ratio and the energy difference. Figure 2 shows the resolved L_{III} M_V component.

The present results are compared with a conventional XANES experiment, measured using fluorescence technique (Hämäläinen *et al* 1989). In that work monochromatic synchrotron radiation, having an incident beam resolution of 1.5 eV was used to measure the cross section of the resonant Raman scattering (RRS) and fluorescence radiation when the incident beam energy was scanned across the Ho L_{III}-edge.

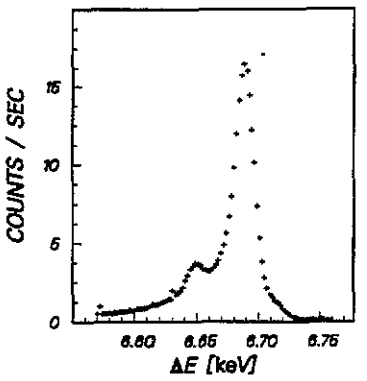

Figure 1. The experimental RRS of holmium including overlapping L_{III} M_{IV} and L_{III} M_V components.

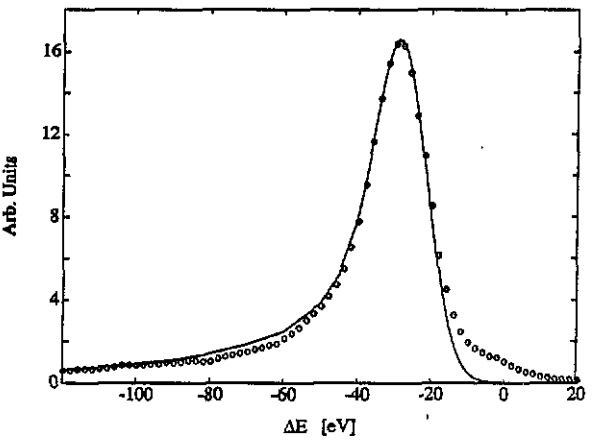

Figure 2. Resolved L_{III} M_V component (open circles). Data shown in figure 1 have been corrected for the effects of background, absorption and solid angle. The energy scale is given relative to the Ho $L\alpha 1$ line position. The L_{III} M_V edge is 23 eV below that energy. Model calculation of the RRS spectrum (full curve) based on constant DOS and a Gaussian white line (FWHM of 5 eV) located at 5.3 eV above the Fermi level. Gaussian resolution function (FWHM of 15 eV) is used.

4. Model calculations

If the density of states (DOS) of the target material is known, equation (1) can be used to calculate the RRS cross section at different incident energies. Furthermore, an integration over the scattered photon energies according to equation (4) leads to the total RRS cross section which can be compared with the measured XANES spectrum. The possible sharp peaks in the DOS are smeared by the inner-shell life-time width but still information about the most apparent features like the white line above the absorption edge can be achieved. On the contrary, the differential RRS cross section (equation (1)) does not include a convolution with the inner-shell lifetime width. Therefore if the instrumental resolution is better than the core level width, sharper features than in conventional XANES spectroscopy can be resolved. These are smeared only by the lifetime width of the upper shell, which is responsible for filling the core

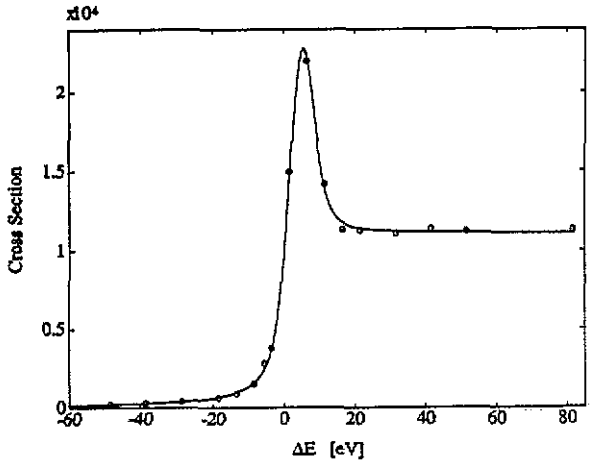

Figure 3. Model calculation (full curve) compared with the fluorescence XANES experiment (open circles).

hole. These widths are appreciably smaller than the core level widths. Another advantage of the high resolution RRS spectroscopy is a better signal-to-background ratio. The measured spectrum is a product of the DOS and Lorentzian tail of the fluorescence line which is more easily subtracted than the absorption edge structure overlapping with the XANES features.

The most apparent feature of the Ho L_{III}-edge XANES spectrum in figure 2 is the white line just above the absorption edge. The theoretical calculations for the density of states of the rare-earth metals are complicated but according to the previous experimental results, all based on the absorption measurements using white spectrum from a conventional x-ray tube (Dubey and Shrivastava 1972, Padalia *et al* 1974, Agarwal and Agarwal 1978), the white line is located at 5.3 eV above the absorption edge and has an FWHM of about 9 eV. To compare the theory with these two different types of experiment a simple constant DOS model was adopted and the white line structure was introduced by adding a single Gaussian peak located at 5.3 eV above the Fermi level. Figures 2 and 3 show the theoretical curves compared with experimental data points when a L_{III}-shell lifetime width of 4.8 eV (Hämäläinen *et al* 1989) is used. The white line in the XANES spectrum is sensitive to the width of the DOS peak and the best fit with the experiment was obtained using FWHM of 5 eV which is clearly smaller than the previous experimental results. The height of the Gaussian peak used in the calculation was 2.3 times the constant DOS level above the Fermi energy.

The theoretical RRS fine structure spectrum shown in figure 2 includes a convolution with a Gaussian having a FWHM of the total instrumental resolution function including the M_V shell lifetime width and the incident energy spread. The small difference on the low energy side of the peak between the theory and the experiment is due to the subtraction procedure of the M_{IV} component and on the high energy side due to the fluorescence caused by the higher energies transmitted through the monochromator.

5. Discussion

Comparison between the model calculation and the experiment in figures 2 and 3

shows surprisingly good agreement. This is partly due to the fact that Ho is an ideal case for this kind of simple density of states model; there is hardly any other structure except the white line in the XANES spectrum. Also one can easily see that the possible XANES structure above the white line (lower energies in figure 2) could be resolved much better in figure 2 than in figure 3 because of the much better signal-to-background ratio. Combined with improved resolution this makes resonant Raman scattering a potential method for XANES studies. The RRS technique would be particularly well suited to studies on magnetic materials using circularly polarized synchrotron radiation, previously carried out using either absorption or fluorescence XANES (Schütz *et al* 1987, Cooper *et al* 1986).

Although the aim of the present work is to propose RRS as an alternative for XANES studies, a few comments on the white line of Ho can be made. The model calculations give the best agreement with the present experiment when the white line is located 5.3 eV above the Fermi level and its FWHM is 5 eV. The location of the white line is in agreement with the previous x-ray absorption experiments (Padalia *et al* 1974, Dubey and Shrivastava 1972) whereas the FWHM is smaller than the value 9.3 eV, reported by Padalia *et al* (1974). Also our fluorescence XANES result in figure 3 shows a FWHM of about 6 eV, again in a close agreement with the model calculation result. In the present case the signal-to-background ratio is much better than in the conventional absorption measurements with an x-ray tube and the determination of the white line width therefore more accurate. Also the position of the white line is more accurate due to the possibility of using known fluorescence energies for energy calibration.

The present work shows the potential of RRS in XANES experiments. To improve the experiment one can consider what can be done to increase the statistical accuracy and to optimize the resolution. The incident monochromatic flux in the present experiment was estimated to be 5×10^9 photon s^{-1} by measuring integrated Bragg reflections from a standard powder sample (Suortti and Jennings 1977). The maximum observed intensity at the peak of the white line was 17 counts per second (cps), and the intensity at the Lorentzian tail, 100 eV from the centre of the line, only about 1 cps. These figures can be improved by increasing the incident flux and the efficiency of the spectrometer. There are obvious improvements of the spectrometer: evacuated or even He–atmosphere beam paths would decrease the absorption in air by a factor of 3, and by the use of a larger detector a comparable increase of the observed flux would be available. With these improvements the resolution of the spectrometer could be brought to the level of 2 eV while maintaining the present efficiency. The incident flux is increased by an order of magnitude when a rotating-anode x-ray generator is used, and another order of magnitude is available from synchrotron sources. At the same time, $\hbar\omega_1$ can be tuned closer to the edge, and polarization can be used for separation of the resonant scattering from the non-resonant A^2 components.

Acknowledgment

The authors are indebted to the Finnish Academy for financial support.

References

Åberg T and Tulkki J 1985 *Atomic Inner-Shell Physics* ed B Crasemann (New York: Plenum) p 419

Agarwal B K and Agarwal B R K 1978 *J. Phys. C: Solid State Phys.* **11** 4223
Bearden J A 1967 *Rev. Mod. Phys.* **39** 78
Bearden J A and Burr A F 1967 *Rev. Mod. Phys.* **39** 125
Cooper M J, Laundy D, Cardwell D A, Timms D N, Holt R S and Clark G 1986 *Phys. Rev.* B **34** 5984
Dubey V S and Shrivastava B D 1972 *Phys. Status Solidi* b **53** K51
Hämäläinen K 1990 *Comment. Phys. Math.* **113** 1
Hämäläinen K, Manninen S, Suortti P, Collins S P, Cooper M J and Laundy D 1989 *J. Phys.: Condens. Matter* **1** 5955
Manninen S, Suortti P, Cooper M J, Chomilier J and Loupias G 1986 *Phys. Rev.* B **34** 8351
Nagasawa H, Mourikis S and Schülke W 1989 *J. Phys. Soc. Japan* **58** 710
Padalia B D, Gupta S N, Vijayavargiya V P and Tripathi B C 1974 *J. Phys. F: Met. Phys.* **4** 938
Pattison P, Suortti P and Weyrich W 1986 *J. Appl. Crystallogr.* **19** 353
Schütz G, Wagner W, Wilhelm W, Kienle P, Zeller R, Frahm R and Materlik G 1987 *Phys. Rev. Lett.* **58** 737
Sparks C J 1974 *Phys. Rev. Lett.* **33** 262
Stern E A 1986 *J. Physique Coll.* **47** C8 3
Suortti P, Eteläniemi V, Hämäläinen K and Manninen S 1987 *J Physique Coll.* **48** C9 831
Suortti P and Jennings L D 1977 *Acta Crystallogr.* A **33** 1012
Suortti P, Pattison P and Weyrich W 1986 *J. Appl. Crystallogr.* **19** 336 and 342
Tohji K and Udagawa Y 1989 *Phys. Rev.* B **39** 7590